DOI:
10.1097/j.pain.0000000000000416

Document Version
Peer reviewed version

Abstract

Severe pain is a common and debilitating complication to metastatic bone cancer. Current analgesics provide insufficient pain relief and often lead to significant adverse effects. In models of cancer-induced bone pain pathological sprouting of sensory fibers at the tumor-bone interface occurs concomitantly to reactive astrocytosis in the dorsal horn of the spinal cord. We observed that CGRP-fiber sprouting in the bone was associated with an increase in CGRP content in sensory neuron cell bodies in the dorsal root ganglia (DRG), and increased basal and activity-evoked release of CGRP from their central terminals in the dorsal horn. Intrathecal administration of a peptide antagonist (α-CGRP8-37) attenuated referred allodynia in the hindpaw ipsilateral to bone cancer. CGRP receptor components (CLR and RAMP1) were up-regulated in dorsal horn neurons and expressed by reactive astrocytes. In primary cultures of astrocyte, CGRP incubation led to a concentration-dependent increase of forskolin-induced cAMP production which was attenuated by pre-treatment with CGRP8-37. Furthermore, CGRP induced ATP release in astrocytes which was inhibited by CGRP8-37. We suggest that the peripheral increase in CGRP content observed in cancer-induced bone pain is mirrored by a central increase in the extracellular levels of CGRP. This increase in CGRP may not only facilitate glutamate-driven neuronal nociceptive signaling, but also act on astrocytic CGRP receptors and lead to release of ATP.

Abstract

Severe pain is a common and debilitating complication to metastatic bone cancer. Current analgesics provide insufficient pain relief and often lead to significant adverse effects. In models of cancer-induced bone pain pathological sprouting of sensory fibers at the tumor-bone interface occurs concomitantly to reactive astrocytosis in the dorsal horn of the spinal cord. We observed that CGRP-fiber sprouting in the bone was associated with an increase in CGRP content in sensory neuron cell bodies in the dorsal root ganglia (DRG), and increased basal and activity-evoked release of CGRP from their central terminals in the dorsal horn. Intrathecal administration of a peptide antagonist (α-CGRP8-37) attenuated referred allodynia in the hindpaw ipsilateral to bone cancer. CGRP receptor components (CLR and RAMP1) were up-regulated in dorsal horn neurons and expressed by reactive astrocytes. In primary cultures of astrocyte, CGRP incubation led to a concentration-dependent increase of forskolin-induced cAMP production which was attenuated by pre-treatment with CGRP8-37. Furthermore, CGRP induced ATP release in astrocytes which was inhibited by CGRP8-37. We suggest that the peripheral increase in CGRP content observed in cancer-induced bone pain is mirrored by a central increase in the extracellular levels of CGRP. This increase in CGRP may not only facilitate glutamate-driven neuronal nociceptive signaling, but also act on astrocytic CGRP receptors and lead to release of ATP.

1. Introduction

Breast, prostate and lung cancers are highly metastatic to the bone. A frequent complication in patients with metastatic disease is cancer-induced bone pain, which starts as intermittent pain that becomes constant with time. Furthermore, the occurrence of breakthrough pain, either spontaneous or due to weight-bearing and movement of the metastatic site, results in poor quality of life in patients [4,27,37].

Recent pre-clinical studies indicate that skeletal pain in primary and metastatic bone cancer includes a neuropathic component. Cancer-induced bone pain is associated with an initial tumor-induced nerve injury of distal processes of sensory fibers, but also sprouting and formation of neuroma-like structures by sensory and sympathetic fibers innervating the tumor-bearing site [3,20]. The current view is that nerve growth factor (NGF) released by endogenous stromal, immune and inflammatory cells drives the sensory fiber ectopic sprouting as this is significantly decreased by early anti-NGF treatment without any effect on either bone destruction or tumor growth [25]. Consistent with the possibility that nerve fiber sprouting contributes to skeletal pain, pre-emptive and sustained anti-NGF treatment attenuates cancer-induced pain behavior whereas late and acute treatment after the appearance of sprouting exerts limited effect [21,26,35]. This suggests that the sprouting of sensory afferents is critical for the development of cancer-induced bone pain, and it has been proposed that such pathological reorganization renders fibers highly sensitive to movement of the tumor-bearing limb and may lead to spontaneous discharge [26].

The bone is mainly innervated by thinly myelinated A-delta sensory fibers and peptidergic C-fibers; the large majority of which express calcitonin gene-related peptide (CGRP)[5]. Accordingly there is a highly significant cancer-induced sprouting of CGRP expressing fibers that is matched by higher numbers of CGRP-positive neuronal cell bodies in dorsal root ganglia (DRG) ipsilateral to the cancer-bearing bone [3,20,29]. Such up-regulation of CGRP in the DRG is the likely product of increased translation which is promoted by retrogradely transported NGF in TrkA-expressing sensory

neurons [31]. Current evidence suggests that whilst more CGRP is shuttled to the peripheral terminals of sensory neurons no changes in CGRP expression can be observed in the dorsal horn ipsilateral to the cancer-bearing bone [19]. However, the dorsal horn pool of CGRP plays a significant role in central mechanisms of nociceptive signaling [24]. In particular the occurrence of referred allodynia, a typical feature of cancer-induced bone pain, suggests the involvement of a state of central sensitization.

Here we tested the hypothesis that an up-regulation of CGRP in sensory neurons innervating the bone is mirrored by an increased release of CGRP from their central terminals in the dorsal horn where CGRP can facilitate neuronal nociceptive signaling in cancer-induced bone pain. Also, as the induction of bone cancer is associated with reactive astrocytes in the dorsal horn [18,19], we investigated whether astrocytes express CGRP receptors and respond to CGRP application.

2. Materials and Methods

2.1. Experimental animals

A total of 77 male C3H/HeN mice (Harlan, Oxfordshire, UK), 5-7 weeks old were used in experiments. Groups of 5 mice were housed at a 12-hour light/dark cycle in a temperature and humidity controlled environment. They were provided with wood-chip bedding material and allowed free access to water and standard diet. All procedures were performed in accordance with the United Kingdom Home Office regulations and followed the guidelines of the International Association for the Study of Pain [43].

2.2. Cancer cell line

NCTC clone 2472 was obtained from the American Type Culture Collection (CCL-11, ATCC, LGC Standards, Middlesex, UK). Cells were cultured in NCTC-135 medium (Sigma-Aldrich, Dorset, UK) supplemented with sodium hydrogen-carbonate and 10% equine serum (Sigma-Aldrich). NCTC 2472

cells used for induction of bone cancer were all in passage 7-10. Cells were harvested at approximately 70% confluency with 1 mM EDTA in 0.1 M phosphate buffered saline (D-PBS, Life Technologies, Paisley, UK), resuspended in Dulbecco's Modified Eagle Medium (D-MEM, Life Technologies), and kept on ice until inoculation.

2.3. Mouse model of cancer-induced bone pain

Bone cancer was induced as previously described [32] with a few modifications. In brief, mice were anaesthetized with isoflurane (IsoFlo®, 2-3% in 1 L/min oxygen) or a mixture of Hypnorm/Hypnovel (VetaPharma Ltd. and Roche, s.c., 2.5 mg/ml fluanisone, 0.079 mg/ml fentanyl citrate, and 1.25 mg/ml midazolam). Post-operative analgesic was provided (Carprieve, Norbrook, 4 mg/kg, s.c.). An incision was made over the right patella and arthrotomy performed to expose the distal femoral epiphysis. A hole was drilled into the medullary cavity with a 30-gauge needle (BD Microlance 3, 30G x 0.5”, VWR, Leicestershire, UK) and 10 µl D-MEM containing 100,000 NCTC 2472 cells was inoculated with an insulin syringe (BD Micro-Fine Plus Insulin Syringes, 0.3 ml, 30G x 8 mm, VWR). The hole was closed with surgical Ethicon bone wax (Harvard Apparatus, Cambridge, UK) and thoroughly irrigated with sterile saline. The skin was closed with surgical wound clips (Scientific Laboratory Supplies Ltd, Nottingham, UK). Sham operated control mice underwent the same operation but were inoculated with D-MEM alone.

2.4. Behavioral testing

Pain-related behaviors were assessed in mice before inoculation of media or cancer cells and at various time intervals after inoculation. Mice were randomly assigned to surgery and treatment groups and the experimenter was blinded to treatments. Tactile allodynia was assessed with a series of calibrated von Frey monofilaments (0.04 g – 4.0 g, Stoelting Co., Wood Dale, IL). The Dixon up and down method was used and a 50% paw withdrawal threshold (PWT) calculated as previously

described [6,11]. Prior to testing, mice were habituated for at least 45 min in test boxes placed upon an elevated metal grid to allow access to the hindpaw. Monofilaments were applied perpendicular to the plantar surface of the hindpaw until a slight bend was observed. Each test started with application of the 0.6 g filament and a response was regarded as positive when a visible reflex paw withdrawal response occurred or the cut-off thresholds of 0.04 g or 4.0 g were reached. Lack of a response led to application of next higher force, while a positive response led to application of next lower force. The weight borne on each hind limb was measured with an Incapacitance Tester (Linton Instruments, Norfolk, UK). Mice were allowed to freely step into the test chamber and encouraged to rest each hind limb on separate transducer pads. Once the mouse was settled in the correct position the weight load of each hind limb was recorded. Mice were forced to change position in between three consecutive measurements by a gentle pull of the tail, and an average weight bearing ratio was calculated as follows: weight placed on the ipsilateral hind limb divided by weight on ipsilateral + contralateral hind limbs. This average ratio was used for statistical analysis. Limb use scores were assigned after examination of the gait of the operated hind limb. Mice were allowed to move freely in a transparent standard cage (365 mm x 207 mm x 140 mm, polycarbonate, Tecniplast UK, London, UK) containing wood chip bedding to allow secure foothold. After a 3 min observation period a score ranging from 4-0 was assigned as follows: 4 = normal gait, 3 = minor limping, 2 = substantial limping, 1 = substantial limping and partial lack of limb use, 0 = total lack of limb use.

2.5. Ex-vivo release of calcitonin gene-related peptide from dorsal horn slices

Extracellular release of CGRP into the dorsal horn was measured in an ex-vivo dorsal horn slice preparation with dorsal roots attached. Only cancer-bearing mice exhibiting a limb use score ≤ 3 were selected for release experiments. Lumbar spinal cords were excised in order to obtain horizontal dorsal horn slices with L3, L4 and L5 dorsal roots attached [8,30]. Slices were mounted in the central compartment of a three-compartment chamber and continuously superfused at 1 ml/min

with oxygenated Krebs' solution (118 mM NaCl, 4 mM KCl, 1.2 mM $MgSO_4$, 1.2 mM KH_2PO_4, 25 mM $NaHCO_3$, 2.5 mM $CaCl_2$, and 11 mM glucose; 95% O_2/5% CO_2) supplemented with 0.1% bovine serum albumin (BSA, Sigma-Aldrich, Dorset, UK) and 2 mg/mL of bacitracin (Sigma-Aldrich) to minimize peptide degradation. The dorsal roots were placed on two electrodes in the lateral compartments and immersed in mineral oil to avoid dehydration. The dorsal horn slices were left to equilibrate for 1 hour prior to collection of 8 ml fractions of superfusates from the central compartment into glass tubes containing acetic acid (0.1 M, Sigma-Aldrich). Three 8 ml fractions were collected to measure the basal outflow of CGRP, followed by one fraction to measure activity-evoked release of CGRP during 8 min electrical stimulation of the dorsal roots at C-fiber strength (20 V, 0.5 ms, 10 Hz) to mimic fibre activity during noxious stimulation. Lastly three fractions were collected to measure the recovery to basal levels of CGRP. The CGRP content in the collected fractions was quantified using a peptide enzyme immunoassay (EIA, α-calcitonin gene-related peptide, Peninsula Laboratories, San Carlos, CA). Briefly the fractions were partially purified and desalted through C18 reverse phase silica gel cartridges (Waters UK, Hertfordshire, UK). Cartridges were conditioned with acetonitrile and 0.1% trifluoroacetic acid (TFA). The sample fraction was loaded and a wash performed with 0.1% TFA, before elution with a mixture of acetonitrile/0.1% TFA (80:20). The eluted samples were dried at 55°C under nitrogen gas. Dried samples were reconstituted in 150 µl assay diluent. 50 µl of CGRP standards (0.01 – 10.00 ng/ml) and 50 µl of unknown samples were run in duplicate according to the manufacture instructions. Absorbance of each sample was measured at 450 nm and CGRP content calculated from the sigmoidal standard curve using nonlinear regression and the paradigm "log(inhibitor) vs. response - Variable slope" (GraphPad Prism v. 5.01, GraphPad Software Inc., La Jolla, CA).

2.6. Drug treatment

Vehicle (saline) or α-CGRP8-37 (dissolved in saline; Bachem AG, Bubendorf, Switzerland) were administered intrathecally (26 gauge needle) at the lumbar enlargement of mice as single bolus injections (5 µl). Cancer and sham operated mice were day 14 randomized into three treatment groups according to their 50% PWT and then treated once daily on days 15-17 after cancer cell inoculation. Cancer operated mice were administered either vehicle (n=10) or α-CGRP8-37 (5 nmol, n=10). Sham operated mice were administered vehicle (n=7). Behavioral testing was performed 60 min post administration. The experimenter was blinded to both operation and treatment groups.

2.7. Immunohistochemistry

IHC in femurs: Mouse femurs inoculated with cancer cells or media were isolated on days 20-22 after surgery. Femurs were cut open at the distal end, fixed in 4% PFA for 48 hours at RT, and then stored in saline at 4°C. They were gently decalcified in 10% EDTA adjusted to pH 7.3 for 2 weeks at 4°C, and cryoprotected in 30% sucrose in 0.1 M PBS prior to embedding in O.C.T. Compound (VWR, Leicestershire, UK). The femurs were serially sectioned along the longitudinal axis into 30 µm sections on a cryostat (Leica CM 3050 S Cryostat) and thaw mounted onto gelatine coated microscope slides. Adjacent sections were subjected to either hematoxylin & eosin (H&E) staining or fluorescent immunohistochemistry. Sections for H&E were stained following standard procedures, dried 1 hour at 60°C, washed 3 times with xylene and mounted with DPX (Sigma-Aldrich, Dorset, UK) mounting medium for imaging. Fluorescent immunohistochemistry was performed as previously described [26]. Sections were blocked for 1 hour in 1% bovine serum albumin (BSA, Sigma-Aldrich) in 0.3% Triton X-100 (Sigma-Aldrich) in 0.1 M phosphate buffered saline (T-PBS), and incubated overnight at RT with sheep anti-CGRP (BML-CA1137, 1:800, Enzo Life Sciences, Exeter, UK), followed by 2 hours incubation with donkey anti-sheep Cy™3-conjugated AffiniPure F(ab')2 fragment (713-166-147, 1:1000, Jackson ImmunoResearch Laboratories, Suffolk, UK). Sections were then mounted with Vectashield mounting medium containing DAPI (Vector Laboratories, Peterborough, UK).

Peptidergic sensory fibres in the femur were visualized by confocal microscopy and images acquired with Zeiss Axio Imager Z2 and LSM 710 system. H&E stained sections were used to microscopically identify bone tissue, bone marrow and cancer cells. Confocal images of adjacent immunofluorescent femur sections were acquired as a Z-stack using a 40x objective and the final image projected from 80 optical sections at 0.25 µm intervals. A total of 4 sham operated mice and 5 cancer-bearing mice were qualitatively inspected.

IHC in dorsal root ganglia: Ipsilateral and contralateral dorsal root ganglia (DRG) L4 were isolated on days 20-22 after cancer cell or sham inoculation. DRG were fixed in 4% paraformaldehyde (PFA) in PBS overnight at 4°C and transferred to 30% sucrose in 0.1 M PBS for cryo-protection (72 hours, 4°C) prior to embedding in O.C.T. Compound. DRG were cut in 15 µm sections on a cryostat and thaw mounted onto SuperFrost plus microscope slides (Menzel Glazer, VWR, Leicestershire, UK). DRG sections were blocked 1 hour in 1% BSA in T-PBS supplemented with 0.1% sodium azide (Sigma-Aldrich, Dorset, UK), and incubated overnight at RT with sheep anti-CGRP (1:800), followed by 2 hours incubation at room temperature with donkey anti-sheep Cy™3-conjugated AffiniPure F(ab')2 fragment (1:1000). After a rinse in PBS sections were incubated 4 hours at RT with mouse anti-βIII tubulin (G172A, 1:1000, Promega, Southampton, UK), followed by 1 hour incubation at RT with goat anti-mouse Alexa Fluor 488 (A-11001, 1:1000, Molecular Probes, Life Technologies , Paisley, UK). After a final rinse in PBS sections were mounted with Vectashield mounting medium with DAPI. CGRP-immunoreactivity (IR) and βIII tubulin-IR were visualized with a Zeiss Axioplan 2 fluorescent microscope. Images were acquired with AxioVision (v. 4.8.3.0, Carl Zeiss MicroImaging GmbH, Jena, Germany). All neuronal cell bodies in the DRGs were identified as positive for βIII tubulin. The intensity of CGRP-IR was measured by densitometry and the areas of the individual cell bodies were determined using ImageJ (version 1.46r, Wayne Rasband, National Institutes of Health, Bethesda, MD). A single cell body was considered high in CGRP-IR when the mean grey level intensity was 50% higher than the average mean grey level calculated for all cells bodies in the section subjected to

entage of cell bodies expressing high level of CGRP-IR was calculated from the total cell numbers in each section. Three sections were analyzed per animal, and a total of 3 sham operated mice and 4 cancer-bearing mice included in the statistical analysis.

IHC in dorsal horn of the spinal cord: Spinal cords from vehicle treated mice were isolated 19 days after cancer cell or sham inoculation. Mice were deeply anaesthetized with pentobarbital (12.5 mg/mouse, i.p., Euthal, Merial) and euthanized by intracardial perfusion with ice cold saline followed by 4% PFA in PBS. Lumbar spinal cords were isolated, post fixed 4 hours in 4% PFA at 4°C, and transferred to 30% sucrose in PBS for cryo-protection (72 hours, 4°C) prior to embedding in O.C.T. Compound. Spinal cords were cut in 20-30 µm transverse sections on a cryostat and either thaw mounted onto SuperFrost microscope slides or stained as free floating sections. Spinal cord sections were blocked for 1 hour in 1% BSA in 0.1-0.3% T-PBS prior to overnight incubation at RT with primary antibody. Primary antibodies included sheep anti-CGRP (1:1000), mouse anti-GFAP (glial fibrillary acidic protein, G6171, 1:500, Sigma-Aldrich, Dorset, UK), mouse anti-NeuN (neuronal nuclei clone A60, MAB377, 1:500, Merch Millipore, Hertfordshire, UK), rabbit anti-CLR (calcitonin receptor-like receptor, C3866, 1:100, Sigma-Aldrich) and rabbit anti-RAMP1 (receptor activity-modifying protein 1, SC11379, 1:50, Santa Cruz Biotechnology, Heidelberg, Germany). Following a rinse in PBS sections were incubated 2 hours at RT with appropriate secondary antibodies, including donkey anti-sheep Cy3-conjugated AffiniPure F(ab')2 fragment (1:800), goat anti-rabbit Alexa Fluor 488 (A-11008, 1:100, Molecular Probes, Life Technologies, Paisley, UK), goat anti-mouse Alexa Fluor 488 (A-11001, 1:1000), chicken anti-goat Alexa Flour 488 (A-21467, 1:1000) and donkey anti-rabbit Alexa Flour 546 (A-10040, 1:1000). All antibodies were applied in 1% BSA in T-PBS. Sections were mounted with Vectashield mounting medium with DAPI. CGRP-IR was visualized with a Zeiss Axioplan 2 fluorescent microscope. Images were acquired with AxioVision (v. 4.8.3.0, Carl Zeiss MicroImaging GmbH, Jena, Germany). CGRP-IR was quantified by densitometry; a total of nine squares measuring an area of 15 µm x 15 µm were placed in the lateral, central and medial part of the superficial dorsal horn. No

differences were found between the three parts, why the mean grey level were averaged for all nine squares and subjected to analysis.

Co-localization of CGRP receptor components CLR and RAMP1 in neurons and astrocytes was determined in the ipsilateral dorsal horn of the spinal cord. Images were acquired with a confocal microscope (Zeiss Axio Imager Z2 and LSM 710 system) using a 20x objective. Analysis was performed in ImageJ (version 1.41, Wayne Rasband, National Institutes of Health, Bethesda, MD) on a predefined area of 400 µm x 600 µm covering laminae I-IV. Neurons were determined as NeuN positive ($NeuN^+$) cells; this stain is seen primarily in the nucleus with a lighter stain in cytoplasm. Astrocytes were determined as GFAP positive ($GFAP^+$) cells. Co-localization was quantified by count of cells positive for NeuN or GFAP alone or cells with co-localization of either CLR or RAMP1, respectively. Identification of lamina was facilitated by DAPI staining of cell nuclei, and only cells with clearly observable nuclei in the focal plane were included in the analysis. For all analyses three sections were analyzed per animal, and a total of 4 sham operated mice and 5 cancer-bearing mice included in the statistical analysis.

2.8. Culture of adult spinal cord astrocytes

Primary cultures of astrocytes were prepared from spinal cords of adult female Sprague-Dawley rats (≈ 150 g, Harlan, Oxfordshire, UK) according to a protocol described by Codeluppi et. al. [9]. Briefly rats were anaesthetized deeply with pentobarbital and euthanized by decapitation. The spinal cord was quickly harvested by hydroextrusion with ice cold 0.1 M PBS and placed in complete medium consisting of basal Astrocyte Medium supplemented with 2% fetal bovine serum, 50 U/ml penicillin, 50 µg/ml streptomycin and Astrocyte Growth Supplement (all reagents from ScienCell Research Laboratories, Carlsbad, CA). Meninges and capillaries were removed and the spinal cord chopped into small pieces using a razor blade. The spinal cord pieces were incubated for 10 min at 37°C in 0.25% w/v trypsin-EDTA (Life Technologies, Paisley, UK), and following a wash in complete

medium they were thoroughly triturated in complete medium. To remove fibroblasts, cell suspensions were pre-adhered for 30 min at 37°C in an uncoated cell culture flask (75 cm^2, Nunc™). The supernatant was then collected and transferred into a poly-D lysine (10 µg/ml) coated cell culture flask. Complete medium was replaced on day 4, 7 and 10. The astrocytes were allowed to grow to almost full confluence. On days 11 and 12 any remaining microglia were removed by a 10 min shake at 1000 rpm followed by an immediate replacement of complete medium. The following day astrocytes were washed with 0.1 M PBS, harvested with 0.25% trypsin-EDTA in 0.1 M PBS, centrifuged at 1000g and re-suspended in complete culture medium. Astrocyte numbers were counted, the astrocytes diluted to the desired concentration in complete medium, and then plated into 24 or 96 well plates depending on the specific assay.

2.9. Assay for cyclic AMP

Astrocytes were cultured in 96 well plates coated with poly-D lysine (10 µg/ml) at a density of 40,000 cells/well. After 48 hours of incubation the culture medium was renewed and the astrocytes were incubated in fresh media for 3 hours prior to experimentation. All astrocytes were pre-treated for 30 min with 3-isobutyl-1-methylxanthine (IBMX, 100 µM, Tocris Bioscience, Abingdon, UK) to prevent the degradation of cAMP, followed by 15 minutes pre-treatment with either vehicle (complete astrocyte medium) or the CGRP peptide antagonist CGRP8-37 (1-10 µM, Tocris Bioscience).Then astrocytes were incubated for 15 minutes with vehicle, forskolin (1 µM, Tocris Bioscience), CGRP (1 – 1000 nM, Alpha Diagnostic Intl Inc., Nottingham, UK), or CGRP8-37 (10 µM). Each treatment was performed in triplicate. All drugs were dissolved in astrocyte complete media from stock solutions and supplemented with forskolin (1 µM) to activate adenylate cyclase and induce formation of detectable levels of cAMP. At the end of treatments media were removed, lysis buffer (100 µL) was added to each well and incubated for 30 minutes at 37°C. cAMP was measured in lysates by competitive immunoassay (cAMP-Screen® ELISA System, Applied Biosystems, Bedford,

MA). A standard curve (0.006 – 6,000 pmol) and unknown samples were run in triplicate according to the manufacture's instruction. Bioluminescence was measured with a luminometer (SpectraMax 340PC384, Molecular Devises LLC, Berkshire, UK), and cAMP concentrations in unknown samples were calculated from the standard curve using linear regression.

2.10. Assay for ATP release

Astrocytes were cultured in 24 well plates coated with poly-D lysine (10 μg/ml) at a density of 25,000 cells/well. After 48 hours of incubation the culture medium was renewed and the astrocytes incubated for 3 hours in fresh media prior to experimentation. Astrocytes were pre-treated for 15 minutes with vehicle or the CGRP peptide antagonist CGRP8-37 (10 μM, Tocris Bioscience, Abingdon, UK). Then astrocytes were incubated for 15 min with CGRP (1000 nM, Alpha Diagnostic Intl Inc., Nottingham, UK), glutamate (1 mM, Sigma-Aldrich, Dorset, UK), or stimulated mechanically (three careful flushes of cells). Each treatment was performed in eight wells. All drugs were dissolved in astrocyte complete media from stock solutions and supplemented with the ecto-ATPase inhibitor ARL 67156 (100 μM, Sigma-Aldrich). At the end of treatments media were removed and ATP content measured with a CellTiter-Glo® Luminescent Cell Viability Assay (Promega, Southampton, UK). An ATP standard curve (10^{-4} – 10^{-13} M) was run in triplicate and unknown samples in duplicate according to the manufacture's instruction. Bioluminescence was measured with a luminometer. ATP concentrations in unknown samples were calculated from the standard curve using linear regression and were normalized to vehicle.

2.11. Statistical analysis

Data are presented as mean ± standard error of mean (SEM). Statistical analysis was performed using GraphPad Prism (v. 5.01 for Windows, GraphPad Software Inc., La Jolla, CA). Immunohistochemical data were analyzed with either two-way or one-way analysis of variance

followed by Bonferroni or Newman-Keuls multiple comparison test, respectively. Student's t-test was used for analysis of co-localization of CGRP receptor components in neurons and astrocytes. Extracellular CGRP release was analyzed with two-way ANOVA followed by Bonferroni's post-test. Student's t-test was used to compare individual fractions. Behavioral data was analyzed with two-way ANOVA followed by Bonferroni's post-test. Analysis of cAMP generation and ATP release were performed with one-way ANOVA followed by Dunnett's multiple comparison test or Newman-Keuls multiple comparison test. For all statistical analyses, a probability value of $P < 0.05$ was considered significant.

3. Results

3.1. Sprouting of peptidergic sensory fibers in cancer cell inoculated femurs.

Osteosarcoma is an osteolytic bone cancer that induces substantial bone resorption [32], and has been associated with sprouting of peptidergic $CGRP^+$ fibers in the C3H mouse model of cancer-induced bone pain [26]. Consistently, we observed sprouting of CGRP positive fibers in cancer-bearing femurs which were isolated on days 20-22 after cell inoculation (Fig. 1A-C). Femur bones of sham operated mice showed a highly linear morphology of $CGRP^+$ positive fibers (Fig. 1A). In contrast an unorganized sprouting of $CGRP^+$ fibers was observed in the ipsilateral femur bone of cancer-bearing mice (Fig. 1B,C).

3.2. CGRP-IR is increased in small diameter cell bodies in DRG, but not in the superficial dorsal horn of the spinal cord ipsilateral to cancer cell inoculated femurs.

Next we evaluated whether the increase of CGRP-expressing fibers in the cancer-bearing bone was mirrored by peptide changes in the cell bodies of the sensory neurons in the DRG and/or in their central terminals in the dorsal horn of the spinal cord.

L4 DRG and superficial dorsal horn of the L4 segment of the spinal cord were selected for CGRP quantification as significant neurochemical and cellular reorganization have previously been demonstrated at this level in the osteosarcoma model of cancer-induced bone pain [18,32].

As expected, CGRP was mostly expressed by small diameter cells in ipsilateral and contralateral DRG obtained from cancer and sham inoculated mice (Fig. 1D-F). However, at 20-22 days after cancer cell inoculation the percentage of ipsilateral small cell bodies (300-600 μm^2) expressing high CGRP-IR was 88% higher than that in sham DRG (Fig. 1F). Overall, there was a 40% increase in the percentage of ipsilateral DRG cell bodies expressing high CGRP-IR when comparing cancer-bearing mice to sham operated mice (Fig. 1G).

The increased numbers of cells expressing CGRP in L4 DRG was not matched by changes in CGRP-IR expression at the central terminals of primary afferent fibers in either ipsilateral or contralateral dorsal horn of cancer-bearing mice compared to sham operated mice (Fig. 1H-J). Previously, using histochemical techniques, CGRP content in the ipsilateral superficial dorsal horn has been reported as unaltered after induction of cancer-induced bone pain [19]. Therefore, it is conceivable that our method is not sensitive enough to detect an increase in an already CGRP rich area.

3.3. Extracellular CGRP levels are higher in the dorsal horns of mice with cancer-induced bone pain.

As the aim of this study was to evaluate whether central changes in the CGRP system play a role in the development of pain-related behaviors in cancer-induced bone pain, we tested the alternate hypothesis that activity-induced release of CGRP from primary afferent fibers in the dorsal horn might be altered as a result of the increased CGRP content in the ipsilateral DRG cell bodies. Only cancer-bearing mice with a limb use score ≤ 3 were included in the experiment (average score 1.8±0.7 compared to 3.9±0.4 for sham operated mice, $P < 0.001$, data not shown).

Basal and activity-evoked release of CGRP in the dorsal horn was measured using the ex-vivo dorsal horn slice preparation with lumbar dorsal roots attached. Overall, significantly higher levels of extracellular CGRP were measured in slices obtained from cancer-bearing mice compared to sham operated mice ($F[1, 45] = 16.42$, $P > 0.001$, two-way ANOVA). Electrical stimulation of the dorsal roots using parameters that mimic transmission of noxious stimuli resulted in a significant increase of CGRP content in dorsal horn superfusates of cancer-bearing compared to sham operated mice (Fig. 2A). However, the 65% increase over basal level in cancer-bearing mice was not significantly different from the 100% increase over basal level measured in slices from sham operated mice (Fig. 2A). Further analysis revealed that basal and recovery outflow levels were significantly higher in slices from cancer-bearing mice compared to sham operated mice (Fig. 2A).

These data indicate that an increased pool of primary afferent fiber-derived CGRP is available in the spinal cord dorsal horn of cancer-bearing mice under both basal and noxious-like condition.

3.4. Intrathecal administration of CGRP8-37 attenuates mechanical allodynia in mice with cancer-induced bone pain.

To investigate the biological relevance of the increased level of primary afferent fiber-derived CGRP in the dorsal horn of cancer-bearing mice, we tested the analgesic potential of a CGRP peptide antagonist delivered intrathecally at the lumbar spinal cord level.

Significant hypersensitivity to applied mechanical stimulation was detected in hindpaws ipsilateral to the cancer cell inoculated femurs on days 9, 11 and 14-17 after inoculation (Fig 2B,C). Also, a shift was seen in the body weight load on the cancer-bearing hind leg resulting in a significantly decreased weight bearing ratio starting day 14 in cancer-bearing mice as compared to sham operated mice (Fig 2D,E).

Injections of α-CGRP8-37 on days 16 and 17 significantly attenuated mechanical allodynia 60 min after each injection producing a 44% reversal of allodynia as compared to vehicle treated cancer-

bearing mice (Fig. 2C). Injection of α-CGRP8-37 did not significantly attenuate allodynia on day 15 after cancer cell inoculation, although there was a trend towards an increase in the 50% PWT. A similar effect of α-CGRP8-37 was observed in the weight bearing set up with a significant increase in the weight bearing ratio between inoculated and non-inoculated hind leg on days 16 and 17 as compared to vehicle treated cancer-bearing mice (Fig. 2E). Previous experiments in our laboratory have demonstrated that intrathecal injections of α-CGRP8-37 have no effect on pain-related behaviors in sham operated mice (data not shown), thus this group was omitted.

These data suggest that an increased primary afferent fiber input to the dorsal horn results in release of CGRP which may maintain osteosarcoma-induced mechanical allodynia.

3.5. Increased expression of CGRP receptor components CLR and RAMP1 in neurons and astrocytes in the dorsal horn of cancer cell inoculated mice.

In order to provide a site of action for extracellular CGRP, we quantified the cellular expression of CGRP receptor components in the dorsal horn of cancer-bearing and sham operated mice. As expected, the induction of cancer in the bone was associated with the presence of reactive astrocytes ($GFAP^+$ cells) in the ipsilateral dorsal horn of the spinal cord. The expression of the two CGRP receptor components, calcitonin receptor-like receptor (CLR) and receptor activity-modifying protein 1 (RAMP1), was observed in both neurons (Fig. 3A,B) and astrocytes (Fig. 4A,B).

A significant increase was observed in the numbers of neurons co-expressing either CLR or RAMP1 in cancer-bearing mice compared to sham operated mice (Fig 3C,D). Specifically, the expression of both receptor components in neurons nearly doubled in the superficial laminae (I-IV) of cancer-bearing mice compared to sham operated mice.

Alongside neurons, a higher number of $GFAP^+$ cells (astrocytes) were found to express CLR and RAMP1 in cancer-bearing mice compared to sham operated mice (Fig. 4C,D). Yet, as numbers of $GFAP^+$ cells in the dorsal horn of cancer-bearing mice was increased by two-fold the percentage of

astrocytes expressing the CGRP receptor components over the total $GFAP^+$ cell population was similar in the dorsal horn of sham and cancer inoculated mice (Fig. 4C,D). Notably, the increased numbers of $GFAP^+$ cells does not reflect an increase of astrocyte numbers, but rather their transformation into a reactive state [36]. Thus, we suggest that reactive astrocytes carry CGRP receptors which could respond to the increased level of extracellular CGRP in the dorsal horn of cancer-bearing mice.

3.6. Cultured adult rat spinal cord astrocytes respond functionally to treatment with CGRP.

Whether CGRP receptors in astrocytes respond functionally to CGRP was investigated by measuring the generation of cAMP in primary cultures of astrocytes isolated from adult rat spinal cords.

CGRP application to cultured astrocytes resulted in a concentration dependent increase in cAMP generation, with a significant increase at 100 and 1000 nM compared to vehicle (Fig. 5A). Pre-treatment with the CGRP peptide antagonist CGRP8-37 (1-10 µM,) significantly attenuated the generation of cAMP in response to 100 nM CGRP (Fig. 5A). CGRP8-37 itself had no effect on cAMP generation (data not shown). Furthermore, CGRP stimulation (1 µM) resulted in a two-fold increase in ATP release, which could be attenuated by CGRP8-37 (Fig. 5B).

Together, these data indicate the expression of functional CGRP receptors on spinal cord astrocytes which could respond to the increased extracellular CGRP in the dorsal horn of cancer bearing mice.

4. Discussion

We provide evidence for increased levels of extracellular CGRP in the dorsal horn of the lumbar spinal cord in mice with cancer-induced bone pain. Cancer-bearing mice displayed spontaneous pain-like behavior as well as referred allodynia. Specifically, we observed that in dorsal

horn superfusates obtained from cancer-bearing mice overall CGRP levels were significantly higher than in slices from sham operated mice, and accordingly activity-evoked release of this peptide reached values 58% higher than in sham operated mice. However, the primary afferent fiber activity-evoked release of CGRP over basal levels was not different in cancer-bearing mice and sham operated mice, respectively. Therefore, we conclude, as a result of basal levels of CGRP being higher under cancer-induced bone pain conditions, that overall CGRP extracellular levels are increased in the dorsal horn.

The increase of extracellular CGRP in the spinal cord was mirrored by significant sprouting of CGRP-expressing fibers innervating the metastatic site. The original sources of peripheral and central CGRP pools are the cell bodies of sensory neurons in the lumbar DRG, and we confirmed that larger numbers of DRG (L4) neuronal cell bodies expressed high CGRP content ipsilateral to the cancer-bearing bone.

Current evidence suggests that NGF is required for sensory fiber sprouting in skeletal bone affected by cancer, and blockage of peripheral NGF impairs the occurrence of cancer-induced bone pain [21,26,35]. Furthermore, peptidergic fibers express receptors for hematopoietic growth factors and respond to granulocyte-macrophage colony-stimulating factors (G-CSF and GM-CSF) by releasing CGRP in the skin adjacent to tumor growth [33]. The observation that neutralization of G-CSF and GM-CSF receptors in the vicinity of the tumor attenuated cancer-induced pain related behaviors and tumor growth, point towards a critical role played by peripheral sensitization of neurons interacting with trophic factors released by tumor and stromal cells [34]. Indeed, tumor cells can deregulate the expression of a unique signature of microRNAs in sensory neurons thereby modulating the expression of pain-related genes which are functionally important in tumor-induced nociceptive hypersensitivity in vivo [1].

Our study adds further details to these peripheral mechanisms, providing evidence that CGRP up-regulation in the DRG is associated with increased availability of this peptide centrally at the first

sensory synapse in the dorsal horn. Here extracellular CGRP can act on CGRP receptors expressed in dorsal horn neurons. We found that CGRP receptor components were present in higher numbers than under normal conditions, and therefore, CGRP may act by enhancing neuronal activation driven by glutamate [24]. In agreement, we found that a CGRP receptor antagonist (α-CGRP8-37) injected at the lumbar spinal cord level attenuated bone cancer-induced allodynia.

Our data indicates that an increased primary afferent input into the dorsal horn is responsible for allodynia in cancer-induced bone pain. Glutamate drives neuronal activation at the spinal level in cancer-induced bone pain through activation of NMDA receptors [17,40]; an effect that is potentiated by CGRP [24]. Thus, cancer-induced bone pain induces a state of central sensitization in which changes in the spinal cord facilitate an increased transmission of nociceptive information. Indeed, the ratio of wide dynamic range (WDR) neurons to nociceptive specific (NS) neurons shifts to 47%:53% from 26%:74% which is observed under normal conditions [38]. Moreover, this increase in WDR neurons over NS neurons is accompanied by increased hyperexcitability of the WDR neurons [12,22]. The observation that intrathecal administration of CGRP increase the activity of WDR neurons further supports a role CGRP and CGRP receptors in driving of central sensitization in cancer-induced bone pain [41].

Furthermore, our evidence suggests that neurons are not the only cells mediating the effect of CGRP. Specifically, we observed that reactive astrocytes in the dorsal horn ipsilateral to the cancer-bearing bone expressed CGRP receptors (CLR/RAMP1). Reactive astrocytes are a typical feature in models of cancer-induced bone pain [18,19], and they may increase extracellular glutamate levels as reactive astrocytes usually decrease the expression of glutamate-uptake transporters [16]. Our data indicate that the activation of CGRP receptors results in cAMP formation and release of ATP from astrocytes, and such mechanisms within the astrocytic network are able to enhance nociceptive signaling.

The neuromodulatory role of ATP can be mediated by purinergic ligand gated ion channels, P2X2/3 and P2X3 receptors, expressed on the central terminals of primary afferent neurons, which transiently enhance the release of presynaptic glutamate [28,39]. Evidence suggests that a rapid non-vesicular release of glutamate can occur in response to P2X7 receptor activation [13], but also in a P2X7 receptor independent manner involving activation of astrocytic P2Y1 receptors [15,42]. Although an astrocytic expression of P2X7 receptors has been questioned [2,7], according to current views these receptors become detectable due to up-regulation in pathological states [10]. Thus, in the spinal cord the increased release of sensory neuron-derived CGRP may activate CGRP receptors expressed on astrocytes leading to release of ATP which can activate both astrocytes (P2X7R) and neurons (P2X3R), thereby facilitating nociception in cancer-induced bone pain. In support of this possibility experimental evidence has demonstrated that spinal application of a P2X7 receptor antagonist attenuated dorsal horn evoked neuronal responses to high-intensity mechanical and thermal stimulation in cancer-bearing mice [14]. Also, intrathecal delivery of a P2X3 receptor antagonist attenuated cancer induced bone pain [23]. Together, these series of evidence indicate that P2X3 and P2X7 receptors may be involved in the central mechanisms driving cancer-induced bone pain, and the findings contribute to the understanding of the intercellular communication between astrocytes and neurons which may hold new therapeutic targets for cancer-induced bone pain.

In conclusion, this study demonstrates that the peripheral increase in CGRP content observed in cancer-induced bone pain is mirrored by a central increase in the extracellular levels of CGRP. This increase in centrally available CGRP may facilitate glutamate-driven neuronal nociceptive signaling, but may also act on astrocytic CGRP receptors and lead to release of ATP.

Acknowledgements

RR Hansen was supported by the Lundbeck Foundation (reference number R93-A8583). M Malcangio wishes to thank the Henry Smith Charity Medical Research (Reference ID 20121872) for financial support. The technical support of John Grist, Carl Hobbs and Clive Gentry is greatly appreciated. The authors declare no competing financial interests.

References

[1] Bali KK, Selvaraj D, Satagopam VP, Lu J, Schneider R, Kuner R. Genome-wide identification and functional analyses of microRNA signatures associated with cancer pain. EMBO Mol Med 2013;5(11):1740-1758.

[2] Bennett MR, Farnell L, Gibson WG. P2X7 regenerative-loop potentiation of glutamate synaptic transmission by microglia and astrocytes. J Theor Biol 2009;261(1):1-16.

[3] Bloom AP, Jimenez-Andrade JM, Taylor RN, Castaneda-Corral G, Kaczmarska MJ, Freeman KT, Coughlin KA, Ghilardi JR, Kuskowski MA, Mantyh PW. Breast cancer-induced bone remodeling, skeletal pain, and sprouting of sensory nerve fibers. J Pain 2011;12(6):698-711.

[4] Caraceni A, Martini C, Zecca E, Portenoy RK, Ashby MA, Hawson G, Jackson KA, Lickiss N, Muirden N, Pisasale M, Moulin D, Schulz VN, Rico Pazo MA, Serrano JA, Andersen H, Henriksen HT, Mejholm I, Sjogren P, Heiskanen T, Kalso E, Pere P, Poyhia R, Vuorinen E, Tigerstedt I, Ruismaki P, Bertolino M, Larue F, Ranchere JY, Hege-Scheuing G, Bowdler I, Helbing F, Kostner E, Radbruch L, Kastrinaki K, Shah S, Vijayaram S, Sharma KS, Devi PS, Jain PN, Ramamani PV, Beny A, Brunelli C, Maltoni M, Mercadante S, Plancarte R, Schug S, Engstrand P, Ovalle AF, Wang X, Alves MF, Abrunhosa MR, Sun WZ, Zhang L, Gazizov A, Vaisman M, Rudoy S, Gomez Sancho M, Vila P, Trelis J, Chaudakshetrin P, Koh ML, Van Dongen RT, Vielvoye-Kerkmeer A, Boswell MV, Elliott T, Hargus E, Lutz L, Working Group of an ITFoCP. Breakthrough pain characteristics and syndromes in patients with cancer pain. An international survey. Palliat Med 2004;18(3):177-183.

[5] Castaneda-Corral G, Jimenez-Andrade JM, Bloom AP, Taylor RN, Mantyh WG, Kaczmarska MJ, Ghilardi JR, Mantyh PW. The majority of myelinated and unmyelinated sensory nerve fibers that innervate bone express the tropomyosin receptor kinase A. Neuroscience 2011;178:196-207.

[6] Chaplan SR, Bach FW, Pogrel JW, Chung JM, Yaksh TL. Quantitative assessment of tactile allodynia in the rat paw. J Neurosci Methods 1994;53(1):55-63.

[7] Chu YX, Zhang Y, Zhang YQ, Zhao ZQ. Involvement of microglial P2X7 receptors and downstream signaling pathways in long-term potentiation of spinal nociceptive responses. Brain Behav Immun 2010;24(7):1176-1189.

[8] Clark AK, Staniland AA, Marchand F, Kaan TK, McMahon SB, Malcangio M. P2X7-dependent release of interleukin-1beta and nociception in the spinal cord following lipopolysaccharide. J Neurosci 2010;30(2):573-582.

[9] Codeluppi S, Gregory EN, Kjell J, Wigerblad G, Olson L, Svensson CI. Influence of rat substrain and growth conditions on the characteristics of primary cultures of adult rat spinal cord astrocytes. J Neurosci Methods 2011;197(1):118-127.

[10] Cotrina ML, Nedergaard M. Physiological and pathological functions of P2X7 receptor in the spinal cord. Purinergic Signal 2009;5(2):223-232.

[11] Dixon WJ. Efficient analysis of experimental observations. Annu Rev Pharmacol Toxicol 1980;20:441-462.

[12] Donovan-Rodriguez T, Dickenson AH, Urch CE. Gabapentin normalizes spinal neuronal responses that correlate with behavior in a rat model of cancer-induced bone pain. Anesthesiology 2005;102(1):132-140.

[13] Duan S, Anderson CM, Keung EC, Chen Y, Chen Y, Swanson RA. P2X7 receptor-mediated release of excitatory amino acids from astrocytes. J Neurosci 2003;23(4):1320-1328.

[14] Falk S, Schwab SD, Frosig-Jorgensen M, Clausen RP, Dickenson AH, Heegaard AM. P2X7 receptor-mediated analgesia in cancer-induced bone pain. Neuroscience 2015.

[15] Fellin T, Pozzan T, Carmignoto G. Purinergic receptors mediate two distinct glutamate release pathways in hippocampal astrocytes. J Biol Chem 2006;281(7):4274-4284.

[16] Fukamachi S, Furuta A, Ikeda T, Ikenoue T, Kaneoka T, Rothstein JD, Iwaki T. Altered expressions of glutamate transporter subtypes in rat model of neonatal cerebral hypoxia-ischemia. Brain Res Dev Brain Res 2001;132(2):131-139.

[17] Gu X, Zhang J, Ma Z, Wang J, Zhou X, Jin Y, Xia X, Gao Q, Mei F. The role of N-methyl-D-aspartate receptor subunit NR2B in spinal cord in cancer pain. Eur J Pain 2010;14(5):496-502.

[18] Hald A, Nedergaard S, Hansen RR, Ding M, Heegaard AM. Differential activation of spinal cord glial cells in murine models of neuropathic and cancer pain. Eur J Pain 2009;13(2):138-145.

[19] Honore P, Rogers SD, Schwei MJ, Salak-Johnson JL, Luger NM, Sabino MC, Clohisy DR, Mantyh PW. Murine models of inflammatory, neuropathic and cancer pain each generates a unique set of neurochemical changes in the spinal cord and sensory neurons. Neuroscience 2000;98(3):585-598.

[20] Jimenez-Andrade JM, Bloom AP, Stake JI, Mantyh WG, Taylor RN, Freeman KT, Ghilardi JR, Kuskowski MA, Mantyh PW. Pathological sprouting of adult nociceptors in chronic prostate cancer-induced bone pain. J Neurosci 2010;30(44):14649-14656.

[21] Jimenez-Andrade JM, Ghilardi JR, Castaneda-Corral G, Kuskowski MA, Mantyh PW. Preventive or late administration of anti-NGF therapy attenuates tumor-induced nerve sprouting, neuroma formation, and cancer pain. Pain 2011;152(11):2564-2574.

[22] Khasabov SG, Hamamoto DT, Harding-Rose C, Simone DA. Tumor-evoked hyperalgesia and sensitization of nociceptive dorsal horn neurons in a murine model of cancer pain. Brain Res 2007;1180:7-19.

[23] Kaan TK, Yip PK, Patel S, Davies M, Marchand F, Cockayne DA, Nunn PA, Dickenson AH, Ford AP, Zhong Y, Malcangio M, McMahon SB. Systemic blockade of P2X3 and P2X2/3 receptors attenuates bone cancer pain behaviour in rats. Brain 2010;133(9):2549-2564.

[24] Latremoliere A, Woolf CJ. Central sensitization: a generator of pain hypersensitivity by central neural plasticity. J Pain 2009;10(9):895-926.

[25] Mantyh P. Bone cancer pain: causes, consequences, and therapeutic opportunities. Pain 2013;154 Suppl 1:S54-62.

[26] Mantyh WG, Jimenez-Andrade JM, Stake JI, Bloom AP, Kaczmarska MJ, Taylor RN, Freeman KT, Ghilardi JR, Kuskowski MA, Mantyh PW. Blockade of nerve sprouting and neuroma formation markedly attenuates the development of late stage cancer pain. Neuroscience 2010;171(2):588-598.

[27] Mercadante S. Malignant bone pain: pathophysiology and treatment. Pain 1997;69(1-2):1-18.

[28] Nakatsuka T, Tsuzuki K, Ling JX, Sonobe H, Gu JG. Distinct roles of P2X receptors in modulating glutamate release at different primary sensory synapses in rat spinal cord. J Neurophysiol 2003;89(6):3243-3252.

[29] Niiyama Y, Kawamata T, Yamamoto J, Omote K, Namiki A. Bone cancer increases transient receptor potential vanilloid subfamily 1 expression within distinct subpopulations of dorsal root ganglion neurons. Neuroscience 2007;148(2):560-572.

[30] Ogbonna AC, Clark AK, Gentry C, Hobbs C, Malcangio M. Pain-like behaviour and spinal changes in the monosodium iodoacetate model of osteoarthritis in C57Bl/6 mice. Eur J Pain 2013;17(4):514-526.

[31] Pezet S, McMahon SB. Neurotrophins: mediators and modulators of pain. Annu Rev Neurosci 2006;29:507-538.

[32] Schwei MJ, Honore P, Rogers SD, Salak-Johnson JL, Finke MP, Ramnaraine ML, Clohisy DR, Mantyh PW. Neurochemical and cellular reorganization of the spinal cord in a murine model of bone cancer pain. J Neurosci 1999;19(24):10886-10897.

[33] Schweizerhof M, Stosser S, Kurejova M, Njoo C, Gangadharan V, Agarwal N, Schmelz M, Bali KK, Michalski CW, Brugger S, Dickenson A, Simone DA, Kuner R. Hematopoietic colony-stimulating factors mediate tumor-nerve interactions and bone cancer pain. Nat Med 2009;15(7):802-807.

[34] Selvaraj D, Kuner R. Molecular players of tumor-nerve interactions. Pain 2015;156(1):6-7.

[35] Sevcik MA, Ghilardi JR, Peters CM, Lindsay TH, Halvorson KG, Jonas BM, Kubota K, Kuskowski MA, Boustany L, Shelton DL, Mantyh PW. Anti-NGF therapy profoundly reduces bone cancer pain and the accompanying increase in markers of peripheral and central sensitization. Pain 2005;115(1-2):128-141.

[36] Sofroniew MV, Vinters HV. Astrocytes: biology and pathology. Acta Neuropathol 2010;119(1):7-35.

[37] Stromgren AS, Sjogren P, Goldschmidt D, Petersen MA, Pedersen L, Groenvold M. Symptom priority and course of symptomatology in specialized palliative care. J Pain Symptom Manage 2006;31(3):199-206.

[38] Urch CE, Donovan-Rodriguez T, Dickenson AH. Alterations in dorsal horn neurones in a rat model of cancer-induced bone pain. Pain 2003;106(3):347-356.

[39] Vulchanova L, Riedl MS, Shuster SJ, Stone LS, Hargreaves KM, Buell G, Surprenant A, North RA, Elde R. P2X3 is expressed by DRG neurons that terminate in inner lamina II. Eur J Neurosci 1998;10(11):3470-3478.

[40] Xiaoping G, Xiaofang Z, Yaguo Z, Juan Z, Junhua W, Zhengliang M. Involvement of the spinal NMDA receptor/PKCgamma signaling pathway in the development of bone cancer pain. Brain Res 2010;1335:83-90.

[41] Yu LC, Hou JF, Fu FH, Zhang YX. Roles of calcitonin gene-related peptide and its receptors in pain-related behavioral responses in the central nervous system. Neurosci Biobehav Rev 2009;33(8):1185-1191.

[42] Zeng JW, Liu XH, Zhang JH, Wu XG, Ruan HZ. P2Y1 receptor-mediated glutamate release from cultured dorsal spinal cord astrocytes. J Neurochem 2008;106(5):2106-2118.

[43] Zimmermann M. Ethical guidelines for investigations of experimental pain in conscious animals. Pain 1983;16(2):109-110.

Figure Legends

Fig. 1. Sprouting of peptidergic sensory fibers and expression of calcitonin gene-related peptide-immunoreactivity (CGRP-IR) in dorsal root ganglion (DRG) cell bodies and superficial dorsal horns of the spinal cord. (A-C) Representative confocal images of bone sections demonstrating CGRP+ fiber innervation in sham operated and cancer-bearing mice 20-22 days post osteosarcoma cell inoculation. Sprouting of peptidergic sensory nerve fibers is evident in bone sections of cancer-bearing animals, while linear sensory fibers are observed in sham mice. DAPI staining visualizes cell nuclei. (D, E) Representative images of CGRP-IR and beta-III tubulin-IR in L4 DRG isolated 20-22 days post osteosarcoma cell inoculation. (F) Quantification of DRG cell bodies which express high CGRP-IR and distribution by cell size (μm^2). (G) Quantification of the total percentage of DRG cell bodies which express high CGRP-IR. (H, I) Representative images of intracellular CGRP-IR in L4 spinal cord dorsal horns obtained 19 days post osteosarcoma cell inoculation or sham operation. (J) Quantification of CGRP-IR in the superficial dorsal horn. (F) $^{**}P < 0.01$ and $^{+}P < 0.05$ compared to small size cell bodies (300-600 μm^2) ipsilateral in sham operated mice and contralateral in cancer-bearing mice, respectively. (G) $^{*}P < 0.05$ compared to ipsilateral site in sham operated mice and contralateral site in cancer-bearing mice, n = 3-4 in each group, 3 sections per animal. (J) n = 4-5 in each group, 3 sections per animal. All scale bars, 100 µm.

Fig. 2. Higher extracellular levels of CGRP in the dorsal horn of cancer cell inoculated mice and attenuation of pain-related behaviors by intrathecal delivery of a CGRP antagonist. (A) Extracellular CGRP content in dorsal horn superfusates under basal conditions, after noxious-like electrical stimulation of the attached dorsal roots (C-fiber strength, 20V, 0.5ms and 10Hz), and during recovery to basal levels. Lumbar spinal cords were obtained from sham operated and cancer-bearing mice day 20-22 post osteosarcoma cell inoculation. (B, D) Cancer-bearing mice demonstrate mechanical hypersensitivity in the ipsilateral hind paw and reduced weight bearing of the cancer-bearing hind

limb compared to sham operated mice. (C, E) On day 16 and 17 paw withdrawal thresholds (PWT) and weight bearing ratios were increased 60 min after intrathecal (i.t.) injections of the CGRP peptide antagonist α-CGRP8-37 (5 nmol/5 µl) compared to vehicle treated cancer-bearing mice. (B, D) $^{**}P < 0.01$ and $^{***}P < 0.001$ compared to sham operated mice, n = 7-20 in each group. (C, E) $^{*}P < 0.05$ and $^{**}P < 0.01$ compared to vehicle treated cancer-bearing mice, n = 7-10 in each group. BL, baseline.

Fig.3. Increased expression of calcitonin gene-related peptide receptor components CLR and RAMP1 in dorsal horn neurons ipsilateral to the cancer-bearing bone. (A, B) Representative confocal images demonstrating co-localization of neurons ($NeuN^{+}$) and receptor components CLR and RAMP1 in L4 ipsilateral dorsal horn of sham operated and cancer-bearing mice day 19 post osteosarcoma cell inoculation. (C, D) Quantification of the numbers of dorsal horn neurons expressing CLR or RAMP1 in cancer-bearing and sham operated mice. $^{*}P < 0.05$ and $^{***}P < 0.001$, n = 4-5 in each group, 3 sections per animal. Scale bar, 100 µm; scale bar insert, 10 µm. NeuN, neuronal nuclei; CLR, calcitonin-like receptor; RAMP1, receptor activity modifying protein 1.

Fig. 4. Increased expression of calcitonin gene-related peptide receptor components CLR and RAMP1 in astrocytes in the dorsal horn ipsilateral to the cancer-bearing bone. (A, B) Representative images demonstrating co-localization of astrocytes positive for GFAP-IR ($GFAP^{+}$) and receptor components CLR and RAMP1 in L4 ipsilateral dorsal horn of sham operated and cancer-bearing mice. (C, D) Quantification of $GFAP^{+}$ astrocytes and CLR or RAMP1 expression in cancer-bearing mice compared to sham operated mice. No difference was found in the expression of CGRP receptor components per astrocyte in spinal cords from cancer-bearing mice compared to sham operated mice. $^{*}P < 0.05$ and $^{**}P < 0.01$, n = 4-5 in each group, 3 sections per animal. Scale bar, 100 µm; scale bar insert, 10 µm. GFAP, glial fibrillary acidic protein; CLR, calcitonin-like receptor; RAMP1, receptor activity modifying protein 1.

Fig. 5. Cultured adult rat spinal cord astrocytes respond functionally to calcitonin gene-related peptide application. (A) cAMP generation was measured 15 min after stimulation with vehicle, forskolin or CGRP. Pre-treatment with either vehicle or CGRP8-37 was started 15 min before CGRP application. (B) ATP release was determined 15 min after application of vehicle, CGRP, glutamate or mechanical stimulation (3 careful flushes of cells with pipette). Vehicle or CGRP8-37 pre-treatment was started 15 min before CGRP application. (A) $^{**}P < 0.05$ and $^{***}P < 0.001$ compared to stimulation with forskolin 1 µM. $^{\#\#}P < 0.01$ and $^{\#\#\#}P < 0.001$ compared to CGRP (100 nM) supplemented with forskolin (1 µM), n = 3 stimulations per condition, representative of one experiment. (B) $^{*}P < 0.05$, $^{**}P < 0.01$ and $^{***}P < 0.001$ compared to vehicle, n = 6-8 stimulations per condition, data pooled from two separate experiments.

Summary

Increased central levels of extracellular CGRP and CGRP receptors expressed on neurons and astrocytes may facilitate nociception in cancer-induced bone pain.

Figure 1

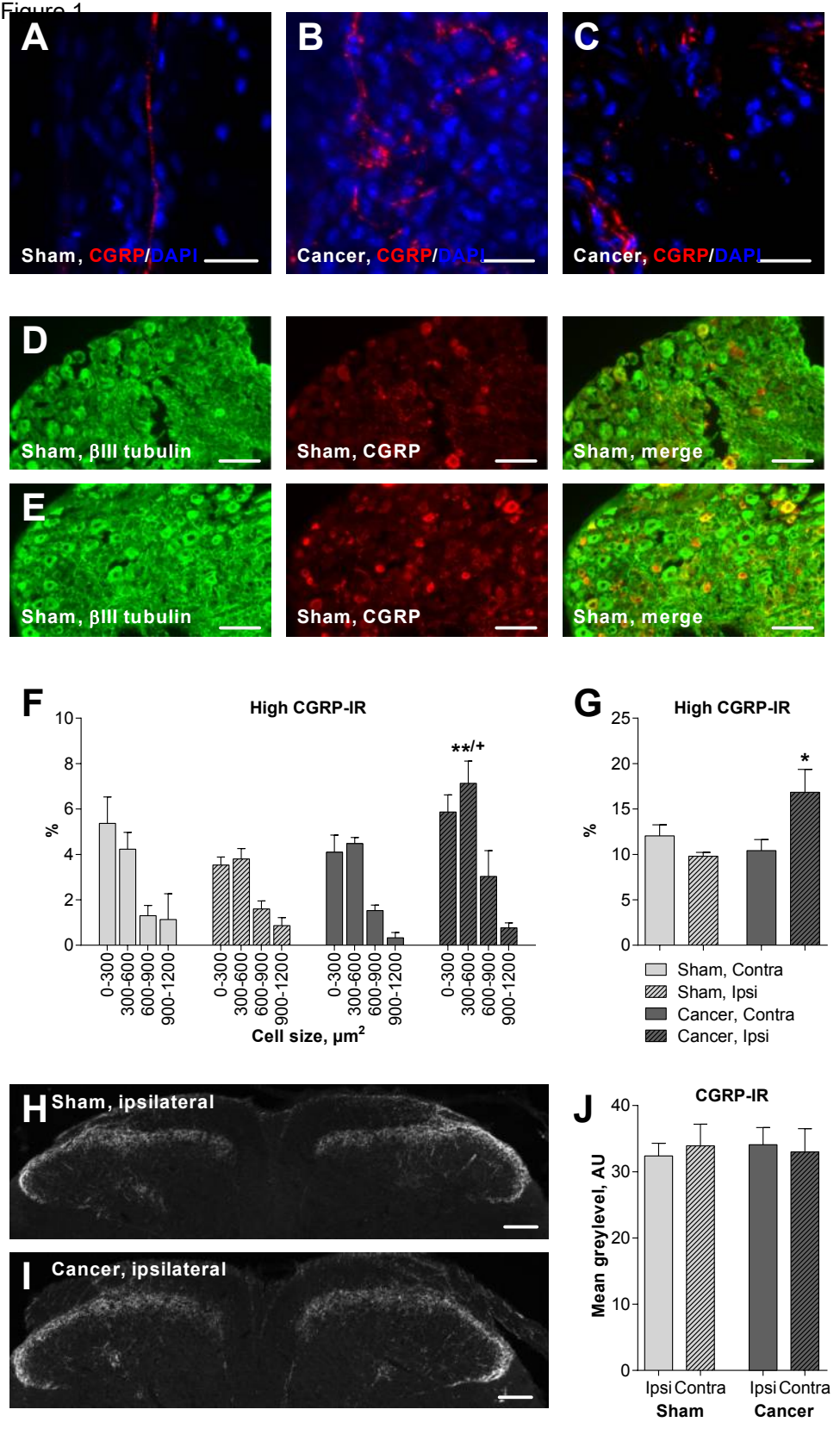
A
Sham, CGRP/DAPI
B
Cancer, CGRP/DAPI
C
Cancer, CGRP/DAPI
D
Sham, βIII tubulin
Sham, CGRP
Sham, merge
E
Sham, βIII tubulin
Sham, CGRP
Sham, merge
F
High CGRP-IR
%
Cell size, μm²
0-300
300-600
600-900
900-1200
**/+
G
High CGRP-IR
%
*
Sham, Contra
Sham, Ipsi
Cancer, Contra
Cancer, Ipsi
H
Sham, ipsilateral
I
Cancer, ipsilateral
J
CGRP-IR
Mean greylevel, AU
Ipsi Contra
Sham
Ipsi Contra
Cancer

Figure 2

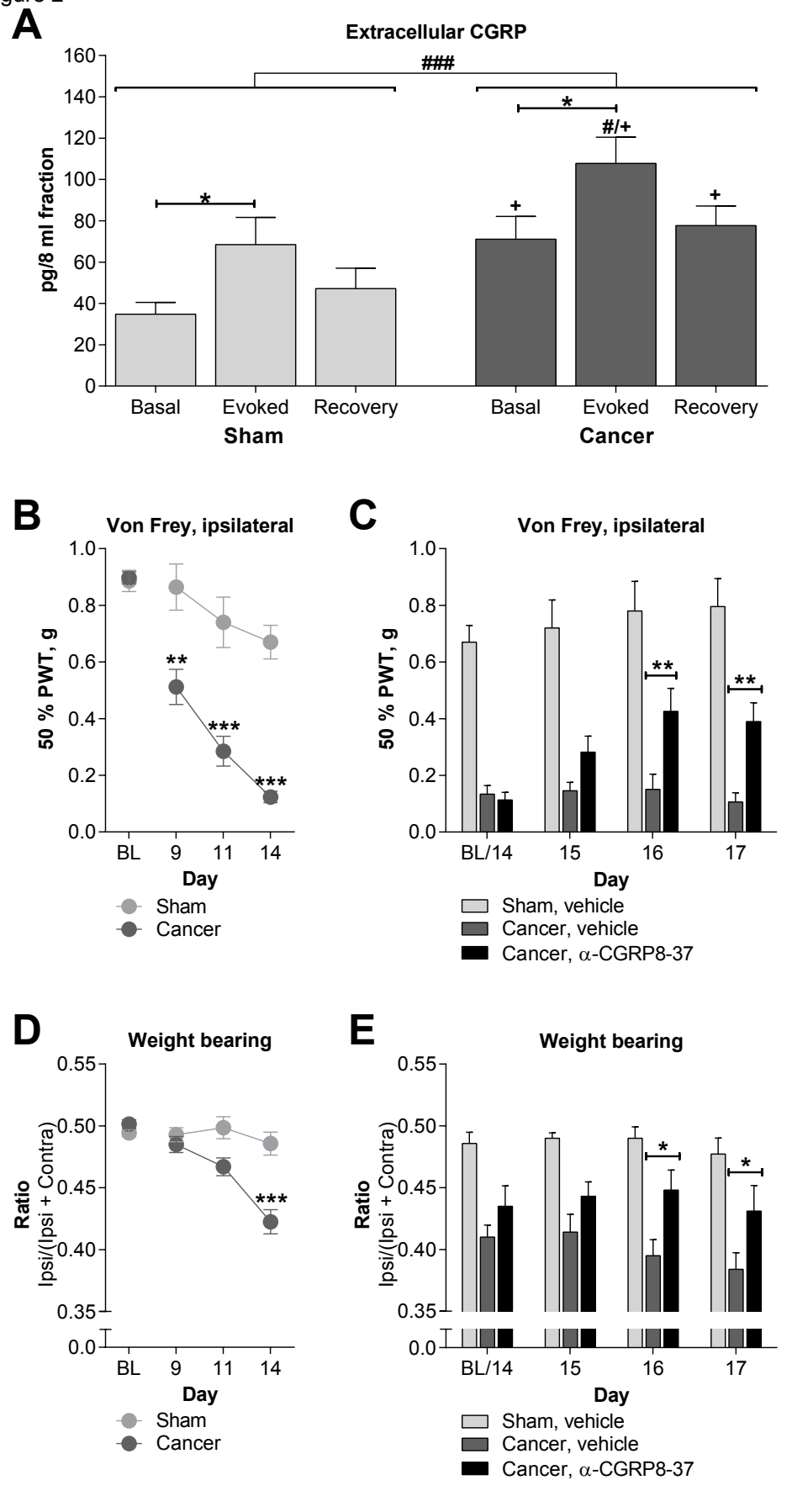
A
Extracellular CGRP
pg/8 ml fraction
###
*
*
#/+
+
+
Basal
Evoked
Recovery
Basal
Evoked
Recovery
Sham
Cancer
B
Von Frey, ipsilateral
50 % PWT, g
**
***
***
BL
9
11
14
Day
Sham
Cancer
C
Von Frey, ipsilateral
50 % PWT, g
**
**
BL/14
15
16
17
Day
Sham, vehicle
Cancer, vehicle
Cancer, α-CGRP8-37
D
Weight bearing
Ratio
Ipsi/(Ipsi + Contra)
***
BL
9
11
14
Day
Sham
Cancer
E
Weight bearing
Ratio
Ipsi/(Ipsi + Contra)
*
*
BL/14
15
16
17
Day
Sham, vehicle
Cancer, vehicle
Cancer, α-CGRP8-37

Figure 3

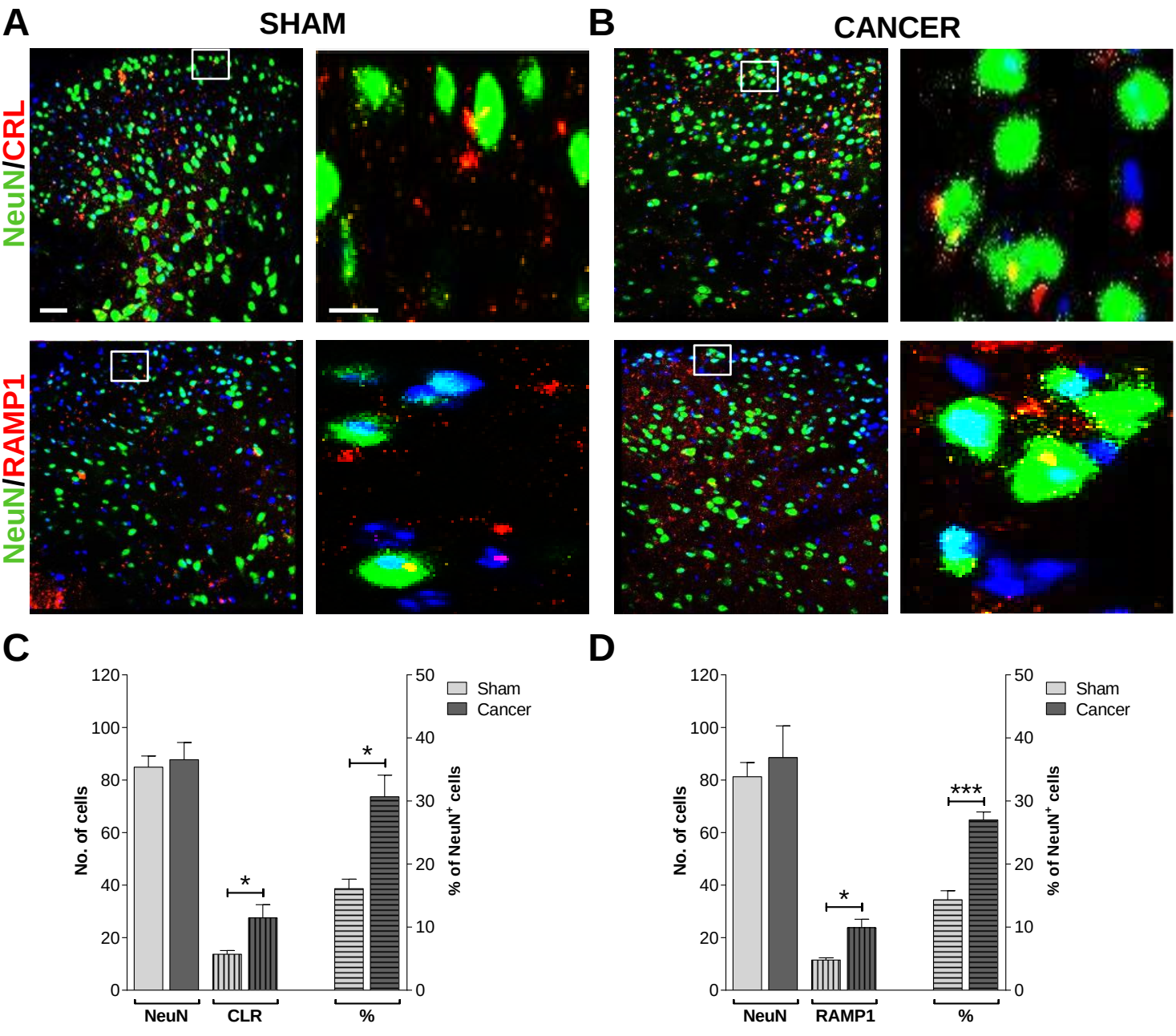
A
SHAM
B
CANCER
NeuN/CRL
NeuN/RAMP1
C
D
No. of cells
% of NeuN+ cells
Sham
Cancer
NeuN
CLR
%
RAMP1
*
***

Figure 4

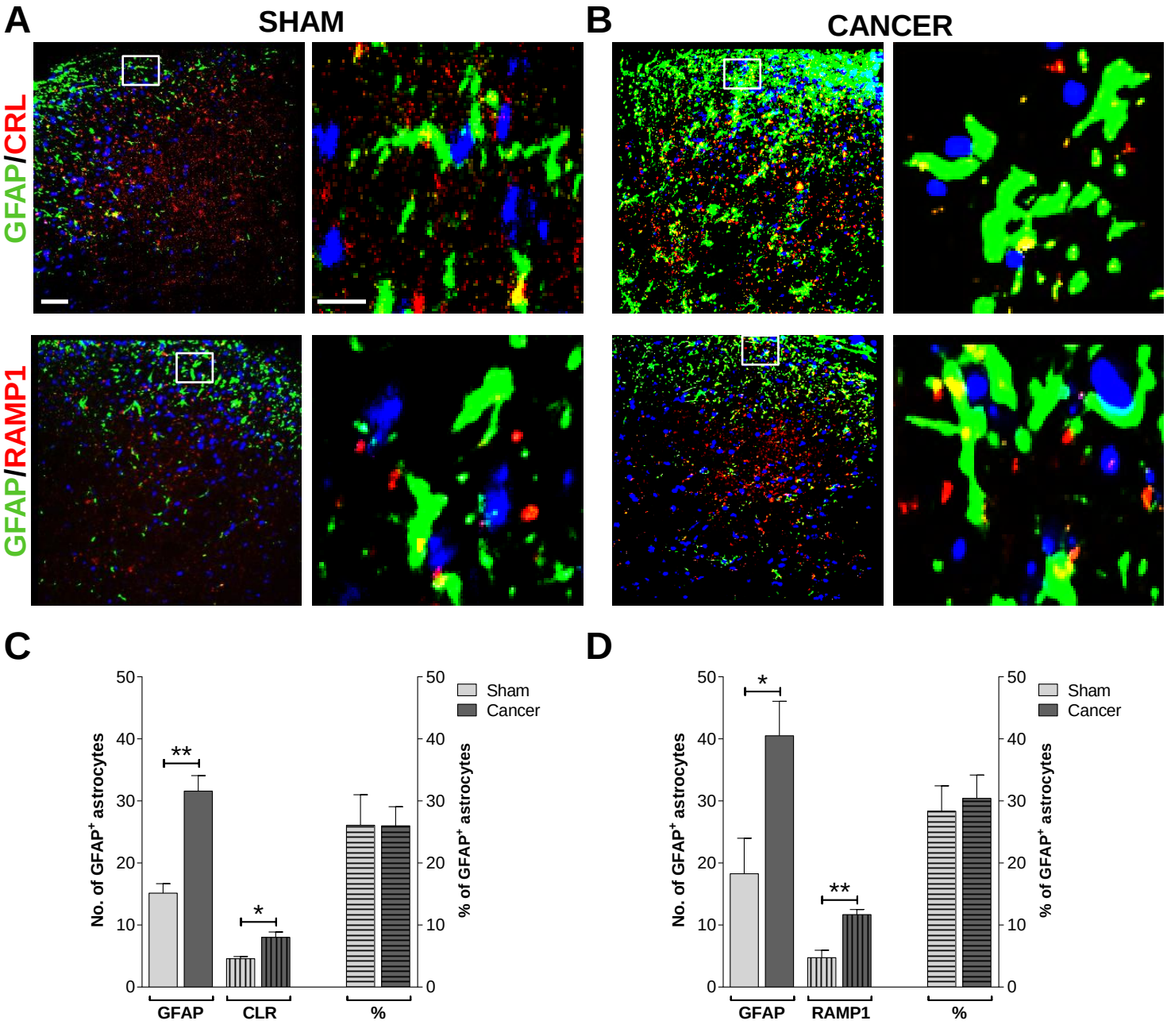
A
SHAM
B
CANCER
GFAP/CRL
GFAP/RAMP1

C
No. of GFAP+ astrocytes
% of GFAP+ astrocytes
Sham
Cancer
**
*
GFAP
CLR
%

D
No. of GFAP+ astrocytes
% of GFAP+ astrocytes
Sham
Cancer
*
**
GFAP
RAMP1
%

Figure 5

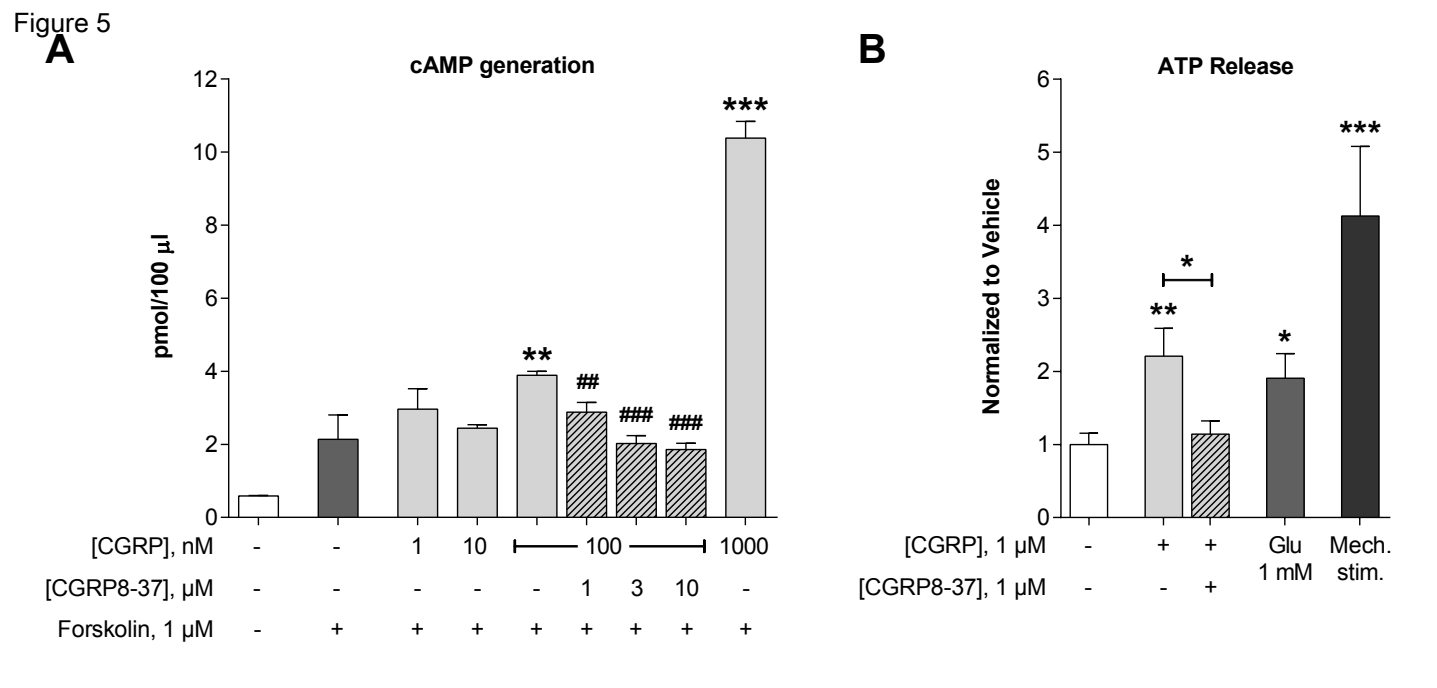
A
cAMP generation
pmol/100 µl
12
10
8
6
4
2
0
**
##
###
###
***
[CGRP], nM - - 1 10 100 1000
[CGRP8-37], µM - - - - - 1 3 10 -
Forskolin, 1 µM - + + + + + + + +
B
ATP Release
Normalized to Vehicle
6
5
4
3
2
1
0
*
**
*
***
[CGRP], 1 µM - + + Glu Mech.
[CGRP8-37], 1 µM - - + 1 mM stim.